

112-Gb/s PAM-4 IM/DD Optical Transmission over 100-km Single Mode Fiber with Linear Equalizer

Shaohua Hu,¹ Jing Zhang,^{1,*} Jianming Tang,² Qun Liu,¹ Wei Jin,² Zhuqiang Zhong,² Roger Giddings,² Jiahao Zhou,¹ Taowei Jin,¹ Xue Zhao,¹ Bo Xu,¹ Xiang Gao,³ and Kun Qiu¹

¹The Key Laboratory of Optical Fiber Sensing and Communications, University of Electronic Science and Technology of China, Chengdu, Sichuan 611731, China

²School of Electronic Engineering, Bangor University, Bangor, LL57 1UT, UK

³Southwest China Institute of Electronic Technology, Chengdu, 610036, China

*Author e-mail address: zhangjing1983@uestc.edu.cn

Abstract: We propose a hybrid linearization algorithm combining the multi-constraint iteration and linear equalization. We experimentally demonstrate a 112-Gb/s PAM-4 signal transmission over 100-km SSMF in IM/DD optical transmission system with one single-ended photodiode.

1. Introduction

The conventional intensity-modulation direct-detection (IM/DD) optical fiber transmission system has simple structure and been deployed in short-reach access network or data-center interconnects. To increase the data rate and transmission distance, techniques such as SSB modulation, Kramers-Kronig receiver and dispersion compensation fiber, have been introduced into IM/DD systems to realize optical field recovery and consequently bring a negligible cost to the already laid communication link [1]. Besides, the digital signal processing, including pre-coding, nonlinear equalization, and high spectrum efficiency modulation, approaches to a ceiling or induce huge complexity to manage severe signal-signal beating interference (SSBI) that results in deep power fadings in the spectrum [2-5].

Recently, a series of G-S algorithms arise the focus on the field linear reception in direct detection system, which retrieves the complex optical field iteratively according to multiple intensity image planes. To form multiple 1-D image planes, dispersive devices have been introduced into the transmission link [6]. For IM/DD system, the simple architecture is its merit for integration and cost so the low-complexity of the digital signal processing (DSP) in the transceiver and the physical layer without hardware changing are preferable. In this regard, there are only two planes in IM/DD systems, i.e., the transmitter-side phase-intensity relationship and the detected optical intensity [7]. Although pre-compensation using G-S algorithms is also effective in channel distortion compensation [8], the post-compensation is flexible to realize optical field recovery. In our previous work, we have proposed a data-aided iterative algorithm and its accelerated version DD-DIA to solve the local optimum problem of G-S algorithm in IM/DD systems [1]. However, the conventional G-S algorithm fails to recover the intensity modulated signal due to the poor global optimum performance as the data rate and transmission distance increases, e.g. 100-Gb/s optical fiber transmission. Besides the SSBI, the band-limited effect is also a typical problem in short-reach IM/DD systems. The conventional G-S algorithms only recover the optical field but have not deal with the band-limited effect.

In this paper, we propose a hybrid G-S multi-constraint iterative algorithm (MCIA) combining with linear equalizer to help find the global optimum solution and mitigate the inter-symbol interference (ISI) due to the band-limited effect. In MCIA, the pilot symbols, decided symbols and redundancy from channel coding are fully utilized to guarantee a promising convergence performance. We insert a feed forward equalizer (FFE) pair into the MCIA in order to mitigate the impact of the residual channel effects on the signal recovery performance. Then, we demonstrate an experimental work of a C-band optical IM/DD transmission using a 112-Gb/s PAM-4 signal transmission over 100-km standard single mode fiber. We find the hybrid MCIA can effectively compensate all the frequency selective power fading and operate well under high optical launch power. It has more than one order of magnitude BER reduction at the optimum launch power compared with Volterra nonlinear equalization and conventional G-S iterative algorithm. Besides, it has 4-dB launch power dynamic range improvement compared with DD-DIA. We find the required inner and outer FFEs of the MCIA iteration has a very short memory length. With the help of the MCIA, the linear equalization is more effective to reduce the BER. To reach the BER of 1×10^{-2} , only 26 cycles of enabled MCIA is introduced.

2. Principle of the Hybrid MCIA

Figure 1(a) shows the principle of the hybrid MCIA. In the receiver, we resample the discrete-time signal by 2 samples per symbol. The initial optical phase $\varphi_{R_init}(m)$ can be a linear function or an all-zero function versus time index, which is multiplied by the detected optical current $I_o(m)$ to form the received signal

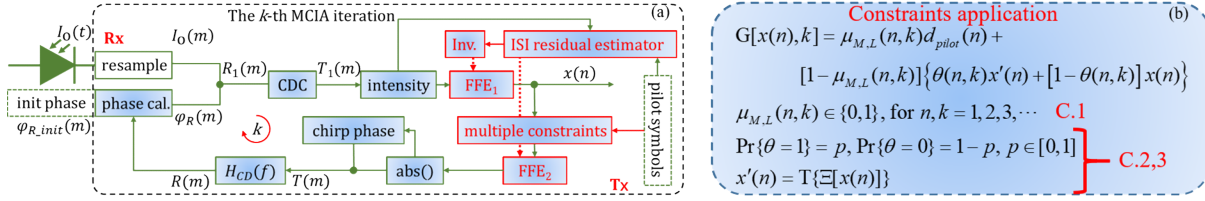


Fig. 1. (a) DSP flowchart of the proposed linearization algorithm. (b) Constraints application.

$R_1(m) = \sqrt{A + I_o(mT_s)} \exp[j\phi_R(m)]$ where A is the bias of the intensity modulator. After intensity-phase combination, the optical signal $R_1(m)$ is digitally back-propagated to generate transmitter-side optical field $T_1(m)$ by frequency-domain inverse CD compensation. After match filtering and down-sampling, we have the symbol sequence $x(n)$.

In MCIA, we apply three constraints on the sequence $x(n)$, as shown in Fig.1 (b). The first constraint is the pilot symbols $d_{pilot}(n)$. By periodically allocating pilot symbols to the information sequence, i.e., the DIA, we can primarily accelerate the convergence performance based on G-S algorithm. The second constraint is the decision process $\Xi[x(n)]$, i.e., DD-DIA. For each decision-directed iteration, the decided symbols are randomly determined with a specific percentage p whether to substitute the continuous distributed values with the decided one. The third constraint is re-utilizing the time-dependence of the binary bit sequence from channel encoding. We can reuse the redundancy of forward error correction (FEC) for decision error correction in DD-DIA immediately after the decision process, i.e., $T\{\Xi[x(n)]\}$ in Fig. 1(b). The latter two constraints do not increase the overhead, so we named the generated decided symbol as pseudo-pilot. To optimize the linearization performance, we usually deploy conventional IA or DIA at the beginning iterations for pre-convergence. To reduce the complexity, the constraints application at part of the following cycles can also be simplified as DD-DIA, DIA, or conventional IA.

After up-sampling and pulse shaping, we obtain the transmitter side intensity modulated signal. According to the specific chirp phase model described in [9], the output optical field $T(m)$ is then digitally forward propagated through the fiber. The updated receiver-side optical field consists of the phase in the forward-propagated complex optical field and the square root of the detected intensity signal. So far, we finish one cycle of MCIA iteration.

From experimental perspective, we insert an inner FFE pair into the MCIA iterations, as shown in Fig. 1(a), to mitigate the impact of the residual memorial effects induced by RF bandwidth limitation and inaccuracy in dispersion estimation on the MCIA linearization performance. The first FFE estimates the residual ISI that MCIA does not compensate and then transforms the backpropagated signal into the transmitted signal. This FFE avoids the under fitting of MCIA on the practical IM/DD channel and improves the accuracy of the pilot insertion and the pseudo-pilot substitution. The second FFE re-introduces the estimated residual ISI on the updated transmitted signal to make the residual effects transparent to the MCIA. The two FFEs inside the iteration make the MCIA well-working under practical case and improve the adaptivity of MCIA. The output of FFE1 can be directly sent to the following blocks. After the hybrid MCIA, we can cascade another simple outer FFE with longer memory length for further equalization. Note that pre-emphasis is necessary to compensate the ISI resulted from the transceiver under back-to-back (B2B) cases.

3. Experiment Setup and Signal Recovery Performance

We transmit a 112-Gb/s PAM-4 signal over 100-km SSMF to verify the signal recovery performance of MCIA. Figure 2(a) shows the experimental setup. An encoded PAM-4 waveform is loaded to an 8-bit DAC operating at 92 GSa/s, which then passes through a radio frequency amplifier (RFA) and is modulated to 1550 nm wavelength using an MZM with the bandwidth of 35 GHz. The external cavity laser has the linewidth of ~ 150 kHz and the output optical power of 10 dBm. The modulated optical signal output from MZM is directly transmitted over 100-km G.652 SSMF with a launch power from 2 to 8 dBm. After fiber transmission, an EDFA is introduced to compensate the fiber loss. Then, a variable optical attenuator (VOA) is cascaded after EDFA to adjust the ROP of the TIA-free single-ended PD with a bandwidth of 40-GHz. The detected optical current is sampled at 200 GSa/s by a digital phosphor oscilloscope (DPO) with a bandwidth of 59 GHz. The transceiver DSP flowchart is illustrated in Fig. 2(b) and (c). The captured electrical spectrum is shown in Fig. 2(d) where 11 deep power fading points exist within the range of 0 to 28 GHz. For better transmission performance, we use a 20-taps FFE for pre-distortion to compensate the bandwidth limitation where the FFE coefficients are calculated at back to back (B2B) case. Note that for DD-DIA and MCIA, the constraints are not applied for every iteration. We alternate the DD-DIA (or MCIA) and conventional IA along the iteration to pursue a better global optimum and a further computational complexity reduction. After the DD-DIA and MCIA, we cascade an FFE, i.e., the outer FFE, to compensate the residual signal distortion resulted from channel modeling imperfection. The electrical spectrum of the recovered signal is depicted

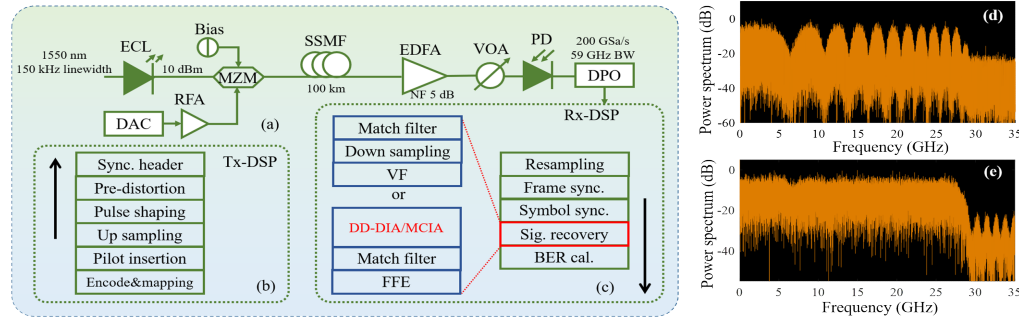


Fig. 2. (a-c) Experiment setup and the DSP flowchart. (d, e) Spectra w/o. and w./ hybrid MCIA.

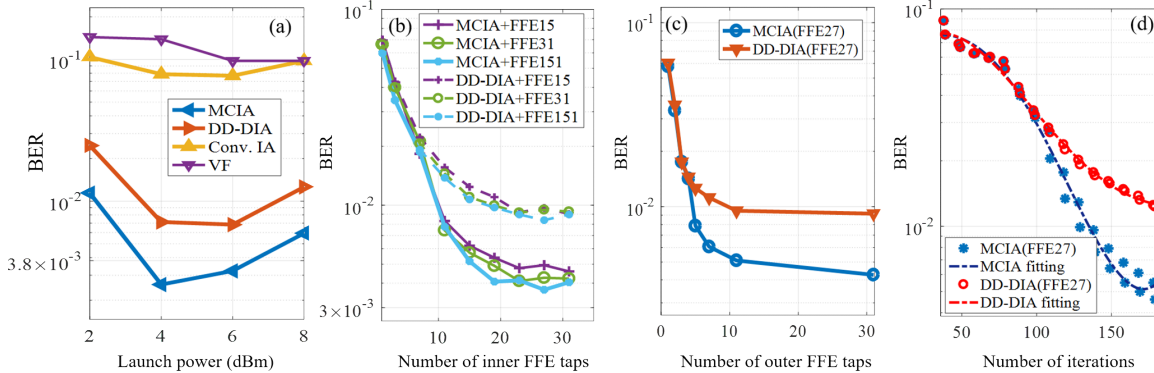


Fig. 3. Experimental signal recovery performance. MCIA+FFE15 represents that an external 15-tap FFE is cascaded by the hybrid MCIA. MCIA(FFE15) represents that a 15-tap inner FFE pair is included in the hybrid MCIA.

in Fig. 2(e) where the launch power and ROP is 6 dBm and 10 dBm, respectively.

Figure 3(a) shows the BER performance versus the launch power aided by different signal recovery algorithms. The VF and conventional IA fails in signal recovery while DD-DIA and MCIA can reduce the BER below 1×10^{-2} . At this BER limit, DD-DIA and MCIA has 4-dB and >8-dB dynamic range. This indicates that the combination of MCIA has higher robustness to the fiber nonlinearity which has potential to support EDFA-free transmission in high launch power applications. To explore the required memory length of the inner and outer FFEs, we calculate the BER versus the number of taps, as shown in Fig. 3(b) and (c) correspondingly. The BER curves verify the necessity of combining the FFE with MCIA in practical transmissions. The inner FFEs can improve the signal recovery performance of MCIA with only 10 to 20 taps. The outer FFE can effectively compensate the residual ISI with 10 taps. Since MCIA has more constraints and the better error correction mechanism, compared with DD-DIA, the FFEs combined with MCIA halves the required number of FFE-taps at the BER of 1×10^{-2} . We show the BER versus the number of iterations in Fig. 3(d) to compare the convergence performance of DD-DIA and MCIA, finding that the MCIA requires 130 cycles of G-S iteration which only includes 26 cycles of MCIA at the BER of 1×10^{-2} . Since the other cycles within the 130 cycles of iteration are the conventional IA, the complexity is reduced further.

4. Conclusions

We have conducted an experiment of a C-band 112-Gb/s 100-km IM/DD PAM-4 optical fiber transmission and verified the effectiveness of the proposed hybrid algorithm combining the MCIA and linear equalizer together. The proposed algorithm can compensate the severe CD-induced SSBI and is robust to channel filtering and fiber nonlinearity with a relative lower complexity.

5. References

- [1] S. Hu et al., *J. Lightwave Technol.* **39**, 2864-2872 (2021).
- [2] X. Li et al., in *Proc. OFC WIA.5* (2016).
- [3] M. Xiang et al., *Opt Express* **26**, 32522-32531 (2018).
- [4] H. Wang et al., *J. Lightwave Technol.* **38**, 5048-5055 (2020).
- [5] Z. Hu and C. Chan, *J. Lightwave Technol.* **38**, 632-641 (2020).
- [6] H. Chen et al., *J. Lightwave Technol.* **38**, 2587-2597 (2020).
- [7] G. Goeger et al., in *Proc. ECOC*, pp. 1-3. (2015).
- [8] X. Wu et al., *Opt. Express* **29**, 24735-24749 (2021).
- [9] C.-C. Wei, *Opt. Express* **20**, 25774-25789 (2012).

This work was supported by National Key Research and Development Program of China (2018YFB1801704), National Science Foundation of China (NSFC) (61871082 and 62111530150), the state Key Laboratory of Advanced Optical Communication Systems and Networks, Shanghai Jiao Tong University (2020GZKF014) and Fundamental Research Funds for the Central Universities (ZYGX2020ZB043 and ZYGX2019J008) and Open Fund of IPOC (BUPT) (No. IPOC2020A011).